6. Situació actual

6. SITUACIÓ ACTUAL

De forma simultània a la realització d'aquest treball de tesi doctoral han aparegut a la literatura nous treballs basats en l'electrodeposició d'aliatges que incorporen molibdè.

D'entre els aliatges binaris, el sistema Ni-Mo ha continuat atraient l'interès dels investigadors. Amb la voluntat d'obtenir materials catalitzadors de la reacció d'evolució d'hidrogen (HER) s'han preparat aliatges Ni-Mo a partir de banys sulfat-citrat [1, 2]. Aquests estudis pretenen correlacionar la composició i estructura dels electrodipòsits amb l'activitat catalitzadora. També s'ha dut a terme la caracterització de capes Ni-Mo obtingudes a partir d'un bany pirofosfat en presència d'agents humectants [3]. Existeix un interès general per obtenir electrodipòsits amorfs/nanocristal·lins atès que l'activitat catalítica se'n veu beneficiada.

D'altra banda, la preparació de capes Co-Mo, ja sigui per electrodeposició [4] o mitjançant mètodes físics [5, 6], ha anat guanyant terreny durant aquests darrers anys. De la mateixa manera que en el cas del sistema Ni-Mo, la voluntat de disposar de materials catalítics de la HER ha esperonat l'interès per electrodipositar Co-Mo. S'ha establert que l'aliatge Co-41%Mo presenta una elevada activitat catalítica i que aquesta pot augmentar amb l'addició de C als dipòsits. Per contra, la preparació de l'aliatge Co-Mo per mètodes físics (polvorització catòdica, IBAD) s'ha dut a terme ressaltant les seves característiques magnètiques. Així, s'han obtingut capes fines Co-13%Mo amb valors d'H_c al voltant de 300 Oe i s'ha investigat la correlació entre estructura i propietats magnètiques.

D'entre els estudis que versen sobre la preparació d'aliatges ternaris, cal destacar els relacionats amb la deposició de capes base cobalt (ja sigui amb incorporacions de níquel superiors a les de molibdè, Co-Ni-Mo, o viceversa, Co-Mo-Ni) i els relacionats amb la deposició de

capes base níquel o base ferro (Ni-Fe-Mo, Ni-Cr-Mo, Fe-Mo-Ni). L'obtenció de Co-Ni-Mo nanocristal·lí mecànicament aliat ha copsat l'interès d'alguns científics per la seva activitat catalítica de la HER en solució alcalina [7]. La relació entre microestructura i propietats magnètiques del sistema Co-Mo-Ni ha estat estudiada per Chu i Wu [8, 9] a partir dels canvis de fase i l'evolució de la microestructura durant el tractament tèrmic dels dipòsits. Aquests investigadors han utilitzat un bany citrat+amoníac a pH=10.5 per electrodipositar capes amb un contingut de molibdè superior al de níquel (14% versus 5%). Pel que fa al segon grup, s'han avaluat les propietats anticorrosió de l'aliatge ternari Ni-Cr-Mo [10] i les propietats catalítiques de la HER d'electrodipòsits Ni-Fe-Mo obtinguts a partir d'un bany citrat+carbonat [11].

En darrer lloc cal dir que han aparegut alguns estudis basats en l'electrodeposició d'aliatges quaternaris que contenen molibdè. Així, per exemple, s'ha aconseguit dipositar Fe-Cr-Ni-Mo a partir d'un bany de clorurs a pH=2 emprant citrat i àcid glicòlic com a agents complexants per acostar els potencials de deposició dels quatre metalls [12]. També s'han preparat capes Ni-Fe-Cr-Mo a partir d'un bany clorur-citrat ateses les seves prometedores propietats magnetoresistives [13]. Els autors d'aquest treball suggereixen que la incorporació de Cr+Mo als dipòsits Ni-Fe redueix la mida del gra, augmenta la resistivitat i la resistència a la corrosió.

De forma paral·lela a l'electrodeposició d'aliatges amb molibdè, també han aparegut diversos treballs basats en l'electrodeposició d'aliatges que contenen tungstè. Per bé que les propietats de resistència al desgast i a la corrosió han continuat atraient l'interès per electrodipositar aliatges binaris de tungstè [14], la possibilitat d'usar-los en sistemes microelectromecànics (MEMS), com a làmines barrera en *ultralarge-scaled integrated systems* (ULSI) o bé com a ànodes en cel·les de combustible de metanol ha començat a captar l'atenció dels investigadors [15-17]. Existeix també un interès general per obtenir

dipòsits de naturalesa amorfa per tal de potenciar la duresa, la ductilitat i la resistència a la corrosió del material [18-21]. Gileadi i Despic, per la seva banda, han esmerçat molt d'esforç en esclarir el mecanisme de codeposició induïda de Ni-W en banys citrat+amoníac a pH bàsic i en la caracterització dels corresponents electrodipòsits [17, 22-25].

A remolc de la publicació dels articles que s'inclouen en aquesta memòria de tesi doctoral, han aparegut darrerament estudis que avalen les nostres propostes mecanístiques. Així, Mascaro i col·laboradors es recolzen en els articles núm. 1, 2 i 3 d'aquesta memòria per corroborar que la presència de lligands policarboxilats en el bany, com ara el citrat, és necessària per a la codeposició d'aliatges de Mo amb metalls del grup del Fe i que, a més, permet mantenir estable el pH durant el procés de deposició [26, 27]. Aquests autors suporten, també, que la reducció de molibdè té lloc via la formació d'una mescla d'òxids/hidròxids de molibdè polivalents. Chassaing *et. al.* han publicat darrerament un estudi basat en la caracterització d'electrodipòsits Ni-Mo nanocristal·lins on fan èmfasi en la necessitat d'aplicar un potencial més negatiu que un cert valor llindar per induir la reducció dels òxids de molibdè a molibdè metàl·lic i, per tant, aconseguir la deposició de l'aliatge [28].

Hem cregut convenient incloure en aquest capítol un *review* que comprèn la preparació, caracterització i aplicació d'aliatges Co-Ni, Co-Mo i Co-Ni-Mo dutes a terme en el nostre grup de recerca. Amb aquest *review* s'ha pretès recollir l'experiència que ha adquirit el grup de recerca en l'electrodeposició d'aliatges base cobalt durant aquests anys, no d'una forma exhaustiva sinó amb la voluntat de mostrar una panoràmica general.

Review: *Electrodeposition of cobalt-based alloys for MEMS*
Enviat per a la seva publicació a la revista Transactions of the Institute of Metal Finishing

6.1 Referències

1. T. SATO, H. TAKAHASHI, E. MATSUBARA, A. MURAMATSU, Mat. Trans. 43 (2002) 1525

2. M. KAROLUS, E. ŁAGIEWKA, J. Alloy Comp. 367 (2004) 235

3. M. DONTEN, H. CESIULIS, Z. STOJEK, Electrochim. Acta 50 (2005) 1405

4. P. R. ZABISNKI, H. NEMOTO, S. MEGURO, K. ASAMI, K. HASHIMOTO, J. Electrochem. Soc. 150 (2003) C717

5. B. ZHAO, G. H. YANG, F. ZENG, F. PAN, Acta Mater. 51 (2003) 5093

6. K. OIKAWA, G. W. QIN, M. SATO, O. KITAKAMI, Y. SHIMADA, J. SATO, K. FUKAMICHI, K. ISHIDA, Appl. Phys. Lett. 83 (2003) 966

7. E. M. ARCE-ESTRADA, V. M. LOPEZ-HIRATA, L. MARTINEZ-LOPEZ, H. J. DORANTES-ROSALES, M. L. SAUCEDO-MUÑOZ, F. HERNÁNDEZ-SANTIAGO, J. Mat. Sci. 38 (2003) 275

8. C.-F. CHU, S.-T. WU, J. Electrochem. Soc. 147 (2000) 2190

9. C.-F. CHU, S.-T. WU, J. Electrochem. Soc. 71 (2001) 248

10. A. C. LLOYD, J. J. NOËL, S. McINTYRE, D. W. SHOESMITH, Electrochim. Acta 49 (2004) 3015

11. F. C. CRNKOVIC, S. A. S. MACHADO, L. A. AVACA, Int. J. Hyd. Energ. 29 (2004) 249

12. A. G. DOLATI, M. GHORBANI, A. AFSHAR, Surf. Coat. Technol. 166 (2003) 105

13. M. GHORBANI, A. IRAJI ZAD, A. DOLATI, R. GHASEMPOUR, J. Alloy Comp. 386 (2005) 43

14. Y. WU, D.-Y. CHANG, D.-S. KIM, S.-C. KWON, Surf. Coat. Technol. 162 (2003) 269

15. T. SHOBBA, S. M. MAYANNA, C. A. C. SEQUEIRA, J. Pow. Sour. 108 (2002) 261

16. M. DONTEN, Z. STOJEK, H. CESIULIS, J. Electrochem. Soc. 150 (2003) C95

17. N. ELIAZ, T. M. SRIDHAR, E. GILEADI, Electrochim. Acta 50 (2005) 2893

18. T. NASU, M. SAKURAI, T. KAMIYAMA, T. USUKI, O. UEMURA, T. YAMASAKI, J. Non-Crys. Solids 312-314 (2002) 319

19. H. WANG, S. YAO, S. MATSUMURA, Surf. Coat. Technol. 157 (2002) 166

20. H. CESIULIS, A. BALTUTIENE, M. DONTEN, M. L. DONTEN, Z. STOJEK, J. Solid State Electrochem. 6 (2002) 237

21. T. NASU, M. SAKURAI, T. KAMIYAMA, T. USUKI, O. UEMURA, K. TOKUMITSU, T. YAMASAKI, Mat. Sci. Eng. A 375-377 (2004) 163

22. O. YOUNES, L. ZHU, Y. ROSENBERG, Y. SHACHAM-DIAMAND, E. GILEADI, Langmuir 17 (2001) 8270

23. O. YOUNES, E. GILEADI, J. Electrochem. Soc. 149 (2002) C100

24. M. D. OBRADOVIC, R. M. STEVANOVIC, A. R. DESPIC, J. Electroanal. Chem. 552 (2003) 185

25. O. YOUNES-METZLER, L. ZHU, E. GILEADI, Electrochim. Acta 48 (2003) 2551

26. L. S. SANCHES, S. H. DOMINGUES, C. ADEMIR, L. H. MASCARO, J. Braz. Chem. Soc. 14 (2003) 556

27. L. S. SANCHES, S. H. DOMINGUES, C. E. B. MARINO, L. H. MASCARO, Electrochem. Commun. 6 (2004) 543

28. E. CHASSAING, N. PORTAIL, A.-F. LEVY, G. WANG, J. Appl. Electrochem. 34 (2004) 1085

Electrodeposition of cobalt-based alloys for MEMS applications

Assumpte: Transactions review
Data: Wed, 24 Aug 2005
De: Sheelagh Campbell [Sheelagh.campbell@port.ac.uk]
A: pellicer@qf.ub.es

Dear Ms. Pellicer,

Electrodeposition of cobalt-based alloys for MEMS applications

I am very pleased to inform you that your paper has been accepted for publication in the Transactions. Both reviewers commented on the quality of the manuscript.

I am intending to include your paper in the September issue of the journal so you will be receiving further communication from the publishers. May I take this opportunity of thanking you for providing me with this excellent review in such a short time. I would be very pleased if you would consider our journal for future publications.

Best wishes

Sheelagh

Dr.Sheelagh A.Campbell,
School of Pharmacy and Biomedical Sciences,
University of Portsmouth,
St.Michael's Building,
White Swan Road,
Portsmouth PO1 2DT, UK

http://www.sci.port.ac.uk/aeg/

Honorary Editor,
Transactions of the Institute of Metal Finishing

Electrodeposition of cobalt-based alloys for MEMS applications

E. Gómez, E. Pellicer*, E. Vallés

Electrodep, Departament de Química Física, Universitat de Barcelona, Martí i Franquès 1, E-08028 Barcelona, Spain.

*Author to whom correspondence should be addressed
e-mail: pellicer@qf.ub.es
Phone: 34 93 403 92 41
Fax: 34 402 12 31

Abstract

The use of cobalt-based alloys in MEMS applications seems feasible and hopeful as these materials are compatible with both planar and bulk technologies involved in MEMS processing. Co-Ni, Co-Mo and Co-Ni-Mo alloys can cover the demand for new materials in the MEMS sector especially in the magnetic actuation field. The route to obtain these alloys must take in consideration the plating bath design, the deposition parameters and the ex-situ characterization of the deposits. A continuous feed-back work based on these items allows tailoring the deposit properties until deposit optimization is achieved. This optimization is not only focused on finding out the more appropriate mechanical and magnetic properties, but on achieving adherent, uniform, low stressed electrodeposited layers.

Keywords: MEMS, electrodeposition, Co-Ni alloy, Co-Mo alloy, Co-Ni-Mo alloy.

1. Introduction

Microsystem technology has become a major research in recent years, as it will allow the generation of a wide variety of technological solutions. Major developments in micro electro mechanical systems (MEMS) have been founded on exploiting micromachining techniques and tools traditionally used for the silicon integrated circuits (ICs) industry. Current research in MEMS explores innovative materials and fabrication techniques combined with traditional semiconductor processes to build a wide range of micro functional devices (sensing, actuating, computing, etc). MEMS will find promising applications in areas such as telecommunications, chemical analysis and biomedical instrumentation. The microworld is a charming and a challenging area of this new century. Ten years ago, the market for micro-machined devices had a large market segment of around US$ 90 million plus

range [1]. Today has become an enabling technology with a worldwide market exceeding US$ 15 billion with a growth rate of at least 20%. This growth is mainly due to automotive and telecommunication applications. Recently there is much work towards realizing practical magnetic-based microactuators for a variety of applications [2-7]. It is desirable that the full integration of ferromagnetic materials in microelectromechanical systems (MEMS) expands their capabilities and can take a small share of this bullish market.

Magnetic microelectromechanical systems (MEMS) actuators have the advantages of low power consumption, long-distance movement and large actuation force. Magnetic films for MEMS applications should meet at least three requirements: reasonable magnetic performance, adaptability to MEMS processing and environmental stability [8]. In order to produce a magnetic force (or actuation) at a specific location, magnetic microactuators should have an inductive component to generate magnetic flux, and a magnetic core to guide the generated flux to the point where actuation takes place. In addition, cores and moving parts must possess high magnetic permeability and good mechanical properties. The major limitation in the fabrication of a magnetic microactuator arises from poor scaling, difficulty in fabrication and high resistive losses, leading to low actuation efficiencies. The usefulness of magnetic microactuators also depends strongly on the application. For example, automotive applications may require much less actuation efficiency than implantable biomedical applications.

Among the large number of microfluidic components realized up to now, micropumps clearly represent the case of a "long runner" in science. The deformation of an object due to an applied external magnetic field can be used to create a remote actuator system by converting a magnetic input signal into a mechanical output [9]. The typical magnetic microactuator is a cantilever or a membrane coated by a magnetostrictive material, which deflects in the presence of an

external magnetic field. Moreover, there is a growing interest in the realization of bidirectionally driven microactuators, which are essential components for optical communication and image process [7]. Bidirectional actuation can be achieved between a permanent magnet and an electromagnet. By altering the exciting direction of the current through the electromagnet, either attractive or repulsive forces can be generated between the magnets. Nowadays, emerging interest of magnetic MEMS appears also in microfluidic analytical separation, in which magnetic separation technique is an ease way to manipulate biomolecules that are immobilized on magnetic particles [10].

Magnets can be integrated into MEMS devices through different techniques such as sputtering, screen printing and electroplating. Sputtering is processed at high vacuum and it is one of the most commonly applied techniques to deposit magnetic films with a thickness of 1-2 μm, but sputtered films with more of 10 μm are much worse than bulk material and the process is time-consuming. Screen-printing produces magnets with relative low cost and the polymer base can be patterned by photolithography [4,6]. Screen-printing is adequate to prepare films of more than 100 μm but it is very difficult to pattern small features. In addition, the mechanical properties of the polymeric material limit its application and the high temperatures needed for curing process is sometimes incompatible with MEMS fabrication. Recent years have witnessed the rapid development of electroplating for fabricating MEMS devices [11,12]. Electroplating is a mature and relative low cost micro-machining technique: most of the deposition processes are compatible with MEMS fabrication and features as small as 1 μm could be obtained. In general electrodeposition is the preferred method, the most recently magnetically actuated microstructure were plate-like structures, which were fabricated by electroplating soft-magnetic materials.

Nickel-iron system is the preferred electrodeposited magnetic material [12-16]. It shows high saturation flux density and low hysteresis and it has been used for many years for magnetic heads. However, Ni-Fe electrodeposition process has been always employed to plate deposits of a well-known *standard* composition (80%Ni-20%Fe), which does not allow to modulate the deposit properties. The cobalt-nickel system appears to be more versatile. From an electrochemical point of view, Co-Ni is deposited according to an anomalous process, the nickel deposition rate being inhibited [17,18]. The coating structure corresponds to a solid solution and the magnetic behaviour can be shifted from hard to soft as nickel-richer deposits are formed. This versatility encouraged us to investigate Co-Ni alloy electrodeposition with the purpose of obtaining improved materials for MEMS.

On the other hand, it is known that molybdenum incorporation in this type of materials improves their soft-magnetic characteristics [14]. For that reason the simultaneous co-deposition of Co, Ni and Mo was attempted, expecting that the beneficial properties of each one of the metals exert a synergic effect on the final properties of the ternary alloy. Molybdenum deposition is unable in aqueous bath, but it is possible to achieve its co-deposition in the presence of a ferromagnetic material [19]. Nickel-molybdenum and cobalt-molybdenum are examples of induced codeposition. In order to gain a better understanding of molybdenum discharge, the incorporation of molybdenum in cobalt deposits was investigated separately.

We report here a review of the processing and characterization of Co-Ni, Co-Mo and Co-Ni-Mo alloys. The electrodeposition process regarding each one of these materials can be manipulated and optimized taking into account three aspects: the reduction process of metal cations in the electrodeposition medium, the kind of the substrate used and the overall morphological, structural and magnetic properties. Metal test structures and components were used to evaluate the properties of the electrodeposited materials. This permits

an iterative process optimization within the fundamental framework described above.

2. Deposition and characterization procedure

To implement a given electrodeposition process in the MEMS fabrication technology some requirements regarding the plating bath are needed. The substrates used must resist the chemical environment and the plating temperature. This is very important when substrates coated with resin are introduced in the bath. A basic electrochemical study is always needed to ascertain the electrodeposition conditions supplying the requirements that the magnetic deposits should have: good adhesion, low stress, corrosion resistance and thermal stability at operating temperatures. This implies a continuous feed-back work, which includes the modification of the bath composition, the stirring conditions, the plating temperature… The use of inert substrates such as vitreous carbon makes easier this basic study. Since the final characteristics of the deposits greatly depend on the deposition parameters, the applied electrodeposition conditions must be tailored depending on the desired application.

For this purpose, the cyclic voltammetric technique was used to ascertain the electrochemical conditions leading to alloy deposition. The study of the voltammetric response allowed setting the appropriate potential range to deposit the cobalt-based alloys under the highest current efficiency. The anodic linear sweep voltammetry (ALSV) was found to be a powerful in-situ characterization method of these alloys. The ALSV experiments were used to oxidise deposits by scanning the potential towards positive values.

Deposit preparation was carried out potentiostatically or galvanostatically. The solution stirring is a critical factor as it must

assure the uniformity of the deposits and a constant composition throughout the thickness.

A study of the properties exhibited by each type of deposits was made: morphology, composition, structure, magnetic and anticorrosion properties. This ex-situ characterisation is essential to ensure that the coatings have the desired properties.

Once the coatings were optimized, their preparation was scaled to substrates of faster technology application such as $Si/SiO_2/Ti/Ni$. P-type 4-40 Ω cm silicon wafers were used. A Ti(1000Å)/Ni(500Å) seed-layer was sputtered on one side of the silicon layer, whereas the other one was insulated by a SiO_2 barrier film to avoid electroplating on both sides. The Ni layer supplies the electrical connection needed to perform the electrodeposition and the Ti layer is needed to improve the adherence between silicon and nickel.

The possibility of depositing on test masks with different shapes and sizes was analysed *(planar technology)*. Different UV-photoresists were patterned on the silicon substrates to get side-walls of a variable height. The filling of the micro-sized features was analysed and the quality of the electrodeposited layer was checked after the resist mold removal.

The possibility of depositing the alloy films in volumetric applications (*bulk technology*) was also tested. The silicon micromachining was performed to provide a microstructure of a specific shape using 25% tetramethylammonium hydroxide (TMAH) as etchant solution at 80ºC. The Ti/Ni seed-layer was sputtered over the silicon 3D structure and, afterwards, the alloy was deposited on top. The total or partial release of the fabricated structures was carried out to check the final quality of the electrodeposited film and its resistance to chemical etching.

Finally, the 'silicon layer-electrodeposited film' pair was subjected to a magnetic actuation test.

More information with regard to the experimental details can be found in the literature [18, 20, 21].

3. Results

3.1. Co-Ni alloy

Co-Ni deposition was carried out from an optimized bath [17, 18]: 0.9 mol dm^{-3} $NiCl_2$ + 0.2 mol dm^{-3} $CoCl_2$ + 30 g dm^{-3} H_3BO_3 + 0.7 g dm^{-3} saccharine. A temperature of 55 ºC was used to favour a high deposition rate.

Since Co-Ni deposition is anomalous-type, the preferential incorporation of cobalt in the deposits occurred. Thus, the Ni(II)/Co(II) ratio in solution must be greater than 4 to achieve a significant nickel incorporation in the deposits. Lower Ni(II)/Co(II) ratios led to quasi-pure cobalt deposits.

The stripping response always showed a single peak. The maximum of the peak shifted towards more positive values as the deposition potential was made more negative (Fig. 1). The comparison between the reduction and oxidation charges revealed that current efficiency was close to 100%. Concurrent chemical analysis showed that the deposits enriched in nickel as the potential was made more negative. According to this, the position of the stripping peak maximum could be linked to the relative metal percentages in the alloy.

Deposit preparation was performed at potentiostatic or galvanostatic conditions at ω=60-100 rpm [22,23]. Co-Ni deposits were silvery-bright, uniform and showed low roughness. A high resolution SEM was needed to image a fine-grained morphology. This morphology was a

consequence of a fast nucleation rate favoured by a high deposition temperature (55ºC).

The saturation magnetization and the coercivity of 15 μm thick Co-Ni films were measured. It was noticed that the saturation magnetization was dependent on the metal percentages in the alloy: it decreased as the nickel percentage increased (Fig 2). When potentiostatic deposition at –800 mV was selected, the deposits consisted of 60 wt% in cobalt and showed a saturation magnetisation of around 120 emu g^{-1}. All the electrodeposited Co-Ni samples prepared showed the characteristics of a soft-magnetic material.

3.2. Co-Mo alloy

Several plating baths were developed in our laboratory to produce cobalt-molybdenum films with Mo percentages ranging 5-13 wt% [21, 24, 25]. Higher Mo percentages were found to decrease significantly the saturation magnetisation of the material. For a start molybdenum incorporation in the deposits could seem complicated taking into account the induced nature of its deposition. However, molybdenum easily deposits when an inductor metal and an appropriate complexing agent (e. g. citrate) are present in the bath. To restrain molybdenum incorporation in the deposits, acidic pH values and low molybdate concentrations are recommended. On the other hand, the deposit quality depended on the [Co(II)]/[citrate] analytical ratio. Best deposits were achieved for [Co(II)]/[citrate]=1.5.

Among the baths we developed, the most promising one contained $C_6H_5Na_3O_7$ 0.2 mol dm^{-3} + $CoSO_4$ 0.3 mol dm^{-3} + Na_2MoO_4 0.012 mol dm^{-3} at pH 4.0. The plating temperature was set at 25ºC.

Three distinct regions were observed in the voltammetric negative scan: a low reduction current attributable to molybdenum oxide formation, a sharp current increase related to Co-Mo alloy deposition

and a third region involving hydrogen coevolution (Fig. 3). In fact, the first region can be distinguished when magnifying the reduction current close to the onset of the reduction process.

Co-Mo deposits prepared form the optimized bath at ω=60 rpm were dark and adherent, with a fluffy morphology and a roughness of 11-60 nm expressed as rms [24]. The molybdenum content depended on the applied potential, so that it decreased as the potential was made more negative.

It has been claimed that the magnetic characteristics of a material depend on its thickness [7]. The measurement of the bulk's magnetic properties does not provide realistic information about the magnetic performance that electrodeposited films would display in MEMS devices. Since thin films are needed for magnetic actuation applications, the magnetic response of 2 μm thick Co-Mo films were studied (Fig. 4). The films showed a strong uniaxial anisotropy given that they spontaneously faced the parallel direction of the applied field when being introduced in a SQUID magnetometer. The incorporation of Mo in cobalt deposits slightly decreased the saturation magnetisation from 138 to 120 emu g^{-1}. Coercivity was clearly lower than that showed by pure-cobalt deposits, so that a softer material was obtained. However, smaller values were achieved in the parallel direction due to the anisotropic characteristics of the material ($H_{c\,||}$ = 70 Oe vs. $H_{c\,\perp}$= 95 Oe). It is known that the structure and how the film grows determine the magnetic performance of a material. Co-Mo deposits showed a close-packed hexagonal structure (hcp) with (100)+(110) preferred orientations. This crystallographic direction and the fact that the deposits grow layer by layer reinforce the magnetic anisotropy.

3.3. Co-Ni-Mo alloy

The design of a Co-Ni-Mo bath to produce ternary films was made taking as a point of reference the optimized Co-Mo bath previously developed. The introduction of few nickel amounts in Co-Mo films was expected to improve the corrosion resistance [26] and the mechanical properties of the material. The composition of the new bath was readjusted to ensure similar cobalt and molybdenum percentages as those obtained in binary films and, at the same time, promote the incorporation of nickel amounts below 20 wt%. A bath containing $C_6H_5Na_3O_7$ 0.2 mol dm^{-3} + $CoSO_4$ 0.05 mol dm^{-3} + $NiSO_4$ 0.25 mol dm^{-3} + Na_2MoO_4 0.005 mol dm^{-3} at pH 4.0 was found to fit the requirements above mentioned [27]. The plating temperature was also set at 25ºC.

A high [Ni(II)]/[Co(II)] analytical ratio was needed to ensure the formation of cobalt-rich alloys due to the anomalous nature of Co-Ni deposition. Moreover, the molybdate discharge was mainly induced by nickel as it was the most abundant inductor metal in solution [28]. The addition of 0.005 mol dm^{-3} saccharine was found to be essential to reduce film stress.

The incorporation of nickel in Co-Mo coatings caused a clear change of the morphology, which evolved from fluffy to cauliflower-like (Fig. 5). Furthermore, grain size and roughness decreased. Both characteristics are responsible to a large extent of the silvery-bright appearance exhibited by Co-Ni-Mo films. On the contrary, significant structural changes were not observed since the hcp structure was maintained.

The anticorrosion properties of Co-Ni-Mo films in a chloride medium were higher than those of Co-Mo films. The presence of nickel in the coatings did not promote a notorious shift of the corrosion potential towards more positive values but decreased the corrosion rate (Fig. 6). Thus, the lifetime of the ternary films would be longer. Moreover,

nickel presence in the coatings increased slightly the microhardness of the material (HU=157 GPa), so that the possibilities of material breakage during operation are less than those expected for Co-Mo films.

2 μm Co-Ni-Mo layers were softer in magnetic terms than homologous Co-Mo layers. The presence of 10-15 wt% nickel in the coatings did not cause a significant decrease of the saturation magnetisation but reduced $H_{c\,||}$ from 70 Oe to 50 Oe and increased the permeability. The Co-Ni-Mo alloy also exhibited a strong uniaxial anisotropy, the magnetisation being easier in the parallel field direction.

3.4. Applications of Co-Ni, Co-Mo and Co-Ni-Mo alloys in MEMS

All alloys were successfully deposited on $Si/SiO_2/Ti/Ni$ substrates. Homogeneous, adherent, dendrite-free deposits were obtained, in which no evidence of movement of their counter parts occurred, even when the spacing-to-opening ratio was high (Fig. 7).

Figure 8 illustrates the possibility of using the deposition of cobalt-based alloys in planar technology. A selective electrodeposition took place in all cases. The alloys filled completely and defined perfectly the conductor cavities, irrespective of the shape and size of the molds. On the other hand, a constant growth rate was achieved in all cases regardless the complexity of the mold geometry. During the removal of the silicon substrate, the electrodeposited free microstructures showed low stress. Thus, the films can be manipulated without producing cracks, thereby increasing the expectations of using them in MEMS actuators.

Furthermore, the alloy films behaved properly when they were subjected to the bulk technology processing. Uniform plating of the overall 3D pieces were achieved when electroplating and no damage was observed when removing the silicon layer (with the TMAH

solution) (Fig. 9). However, Co-Mo films showed greater stress than Co-Ni and Co-Ni-Mo films.

Figure 10 shows micromachined MEMS pieces consisting on a 7-8 μm thick silicon body sputtered with a 1500Å Ti/Ni seed-layer and a 2 μm thick Co-Ni-Mo film deposited on top. Both SEM images prove the electrodeposition capability of plating on shaped substrates. Several experiments were carried out to investigate the performance of 'Co-Ni-Mo valves' under an external magnetic field (Nd-Fe-B magnet). The valves held out several cycles of 30-40 μm bending without being broken. The displacement induced by the magnet was higher as the thickness of the Co-Ni-Mo film increased. Thus, the magnetic response of a microvalve and, generally, of a given MEMS component can be modulated by modifying the electrodeposited film thickness.

4. Conclusions

This review demonstrates the chance of electrodeposited cobalt-based alloys to be implemented in MEMS devices. We report here some examples of this type of materials developed in our laboratory: Co-Ni and Co-Mo as examples of binary alloys and Co-Ni-Mo as an example of ternary alloy. A procedure has been followed in each case to achieve the more appropriate magnetic and mechanical properties. The electrochemical conditions were tailored to obtain uniform and low stressed deposits under a reasonably high current efficiency. The magnetic properties are adequate for magnetic actuation and the mechanical ones ensure that no film breakage occurs when working. The alloy composition was always controlled to get cobalt-rich alloys, therefore ensuring a high saturation magnetization. The incorporation of nickel or molybdenum allowed decreasing the coercivity, leading to soft-magnetic films. Moreover, these metals improved the corrosion resistance of the material. Co-Ni, Co-Mo and Co-Ni-Mo alloys were resistant to chemical etching involved in MEMS fabrication techniques.

The compatibility of these materials with both planar and bulk technologies was verified. Thus, an encouraging MEMS market is opening to cobalt-based alloys.

Acknowledgments

The authors wish to thank the Serveis Cientificotècnics (Universitat de Barcelona) for the use of their equipment. The authors also thank the Centre Nacional de Microelectrònica (CNM-CSIC) for the technological support. This paper was supported by contract MAT 2003-09483-C02-01 from the *Comisión Interministerial de Ciencia y Tecnología (CICYT)*. E. Pellicer also thanks the DURSI of the *Generalitat de Catalunya* for a PhD grant.

References

1. D. Niarchos, *Sensors and Actuators A*, 2003, **109**, 166.

2. W. P. Taylor, O. Brand, M. G. Allen, *J. Microelectromech. Syst.*, 1998, **7**, 181.

3. J. Y. Park, M. G. Allen, *J. Micromech. Microeng.*, 1998, **8**, 307.

4. L. K. Lagorce, O. Brand, M. G. Allen, *IEEE J. Microelectromech. Syst.*, 1999, **8**, 2.

5. T.-S. Chin, *J. Mag. Mag. Mater.*, 2000, **209**, 75.

6. N. Damean, B. A. Parviz, J. Ng Lee, T. Odom, G. M. Whitesides, *J. Micromech. Microeng.*, 2005, **15**, 29.

7. S. Guan, B. J. Nelson, *Sensors and Actuators A*, 2005, **118**, 307.

8. C. H. Ahn, M. G. Allen, *J. Microelectromech. Syst.*, 1993, **2**, 15.

9. W. Wang, Z. Yao, J. C. Chen, J. Fang, *J. Micromech. Microeng.*, 2004, **14**, 1321.

10. J.-W. Choi, T. M. Liakopoulos, C. H. Ahn, *Bionsens. Bioelectron.*, 2001, **16**, 409.

11. B. H. Stark, K. Najafi, *J. Microelectromech. Syst.*, 2004, **13**, 147.

12. D. P. Arnold, F. Cros, I. Zana, D. R. Veazi, M. G. Allen, *J. Microelectromech. Syst.*, 2004, **13**, 791.

13. B. Löchel, A. Maciossek, H. J. Quenzer, B. Wagner, *J. Electrochem. Soc.*, 1996, **143**, 237.

14. W. P. Taylor, M. Schneider, H. Baltes, M. G. Allen: Proc. Int. Conf. on 'Solid-State Sensors and Actuators', Transducers'97, Chicago, 1997, pp.1445-1448.

15. L. T. Romankiw, *Electrochim. Acta*, 1997, **42**, 2985

16. S. D. Leith, D. T. Schwartz, *J. Microelectromech. Syst.*, 1999, **8**, 384.

17. E. Gómez, J. Ramírez, E. Vallés, *J. Appl. Electrochem.*, 1998, **28**, 71.

18. E. Gómez, E. Vallés, *J. Appl. Electrochem.*, 1999, **29**, 805.

19. A. Brenner: *Electrodeposition of Alloys*, vol. 1-2, Academic Press, New York, 1963.

20. E. Gómez, E. Pellicer, E. Vallés, *J. Electroanal. Chem.*, 2003, **556**, 137.

21. E. Gómez, E. Pellicer, E. Vallés, *J. Electroanal. Chem.*, 2004, **568**, 29.

22. M. Duch, J. Esteve, E. Gómez, R. Pérez-Castillejos, E. Vallés, *J. Electrochem. Soc.*, 2002, **149**, C201.

23. M. Duch, J. Esteve, E. Gómez, R. Pérez-Castillejos, E. Vallés, *J. Micromech. Microeng.*, 2002, **12**, 400.

24. E. Gómez, E. Pellicer, E. Vallés, *Electrochem. Commun.*, 2004, **6**, 853.

25. E. Gómez, E. Pellicer, E. Vallés, *Surf. Coat. Technol.*, 2005, **197**, 238.

26. W. Z. Friend: *Corrosion of Nickel and Nickel Alloys*, Wiley-Interscience, New York, 1980, pp. 95-135, 248.

27. E. Gómez, E. Pellicer, E. Vallés, *Electrochem. Commun.*, 2005, **7**, 275.

28. E. Gómez, E. Pellicer, E. Vallés, *J. Electroanal. Chem.*, 2005, **580**, 222.

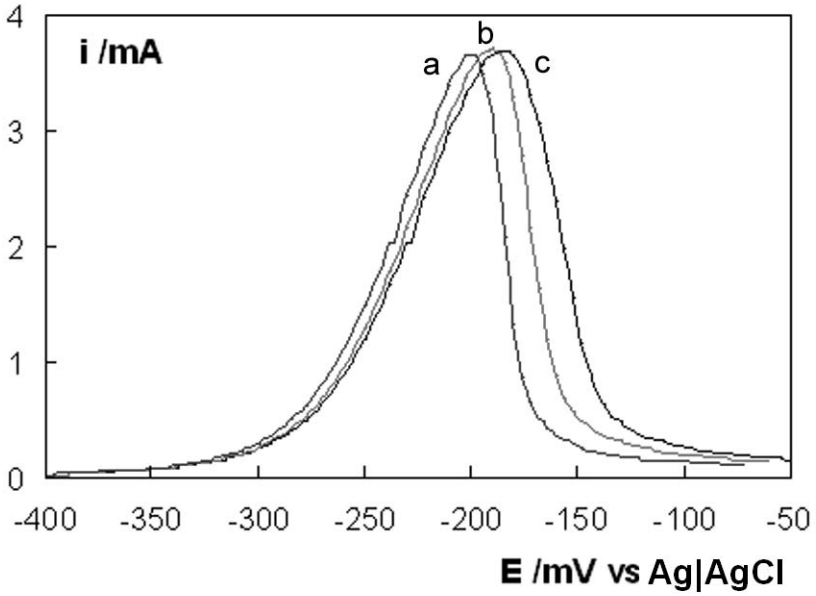

Figure 1. Stripping at 10 mV s^{-1} of Co-Ni deposits obtained under the same deposition charge applying (a) –800, (b) –900 and (c) –1000 mV. Vitreous carbon electrode (0.0314 cm^2), quiescent conditions.

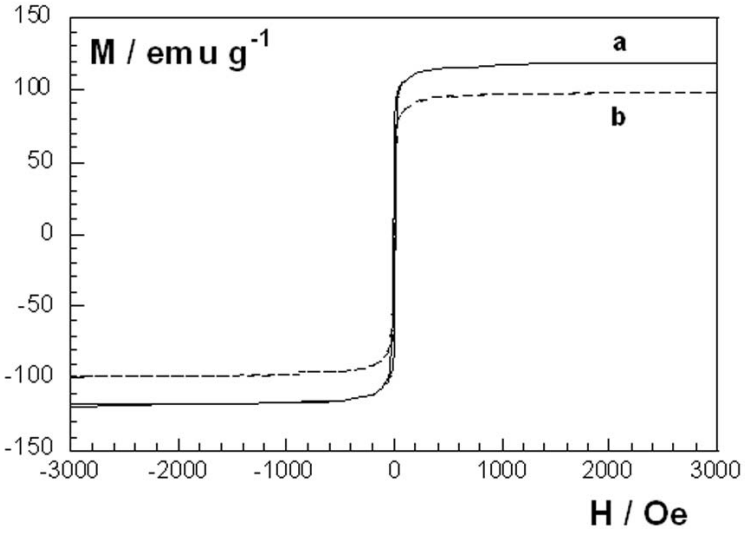

Figure 2. Hysteresis loops of 15 μm thick Co-Ni deposits obtained at (a) –800 mV, 40 wt% Ni and (b) –950 mV, 53 wt% Ni.

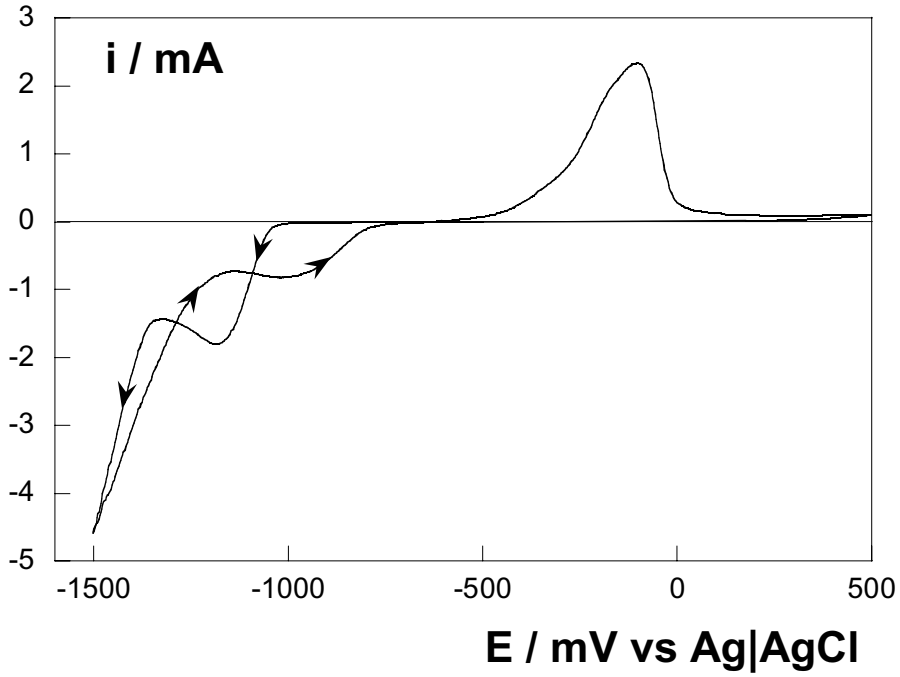

Figure 3. Cyclic voltammetry recorded at 50 mV s^{-1} from a Co-Mo bath on vitreous carbon electrode (0.0314 cm^2). Cathodic limit=–1500 mV, quiescent conditions.

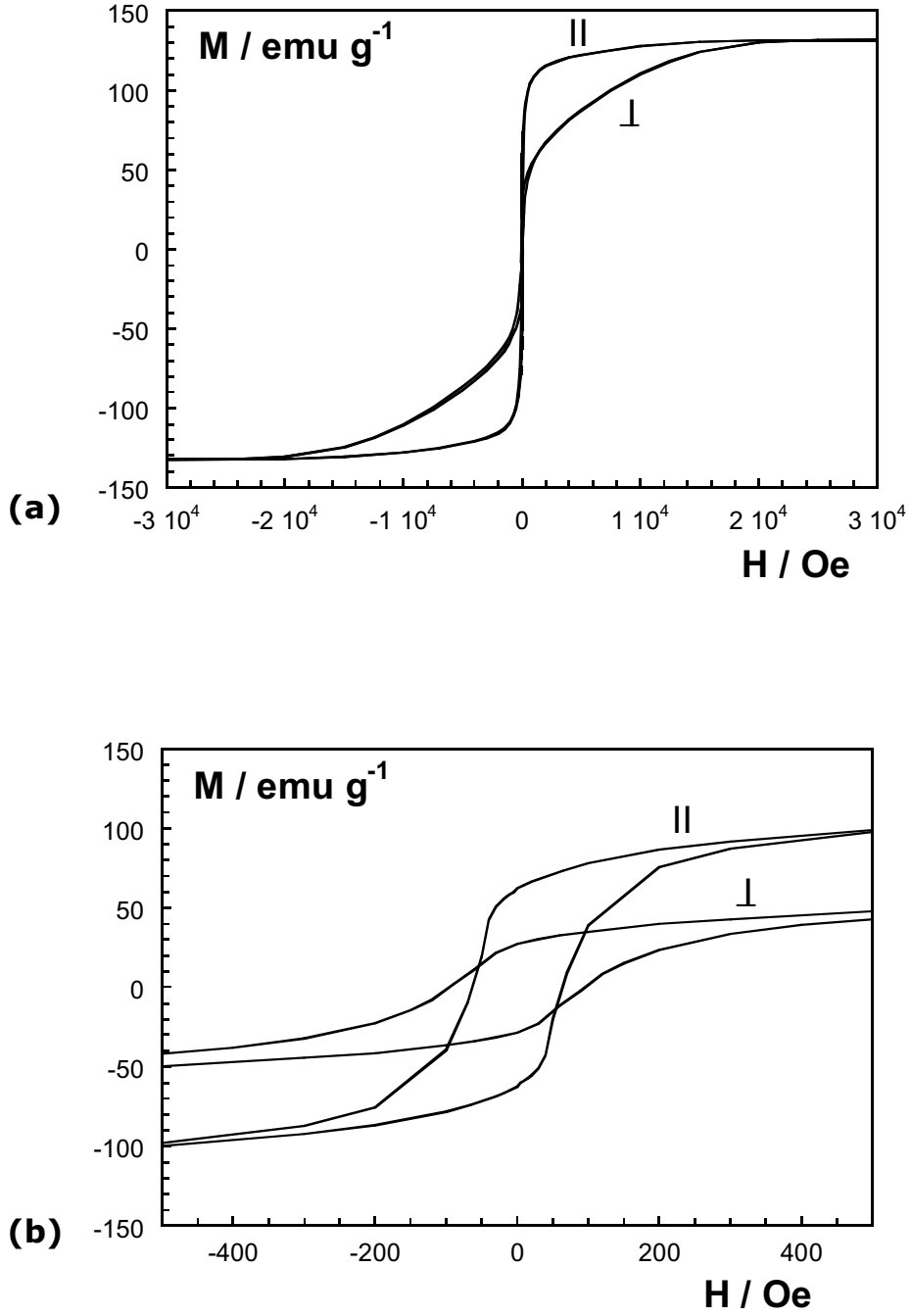

Figure 4. (a) Parallel and perpendicular hysteresis loops and (b) magnified detail of a 2 μm thick Co-11 wt% Mo deposit.

(a)

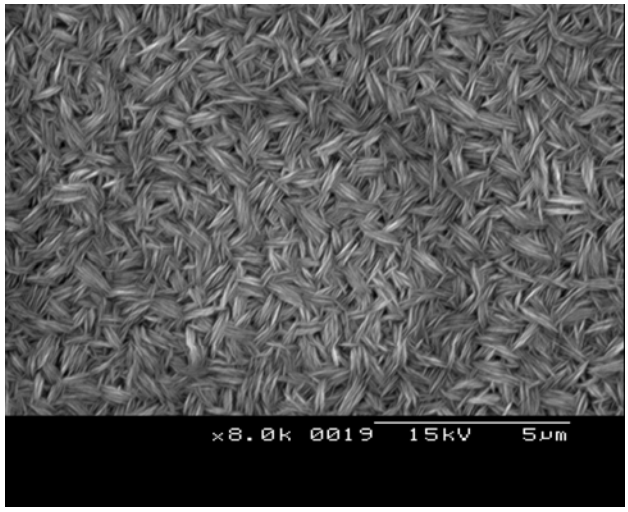

(b)

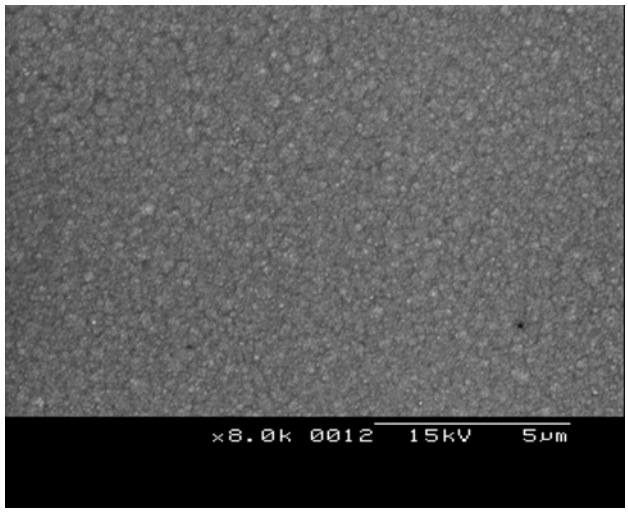

Figure 5. SEM images of (a) Co-11wt% Mo and (b) Co-12wt% Ni-13wt% Mo films.

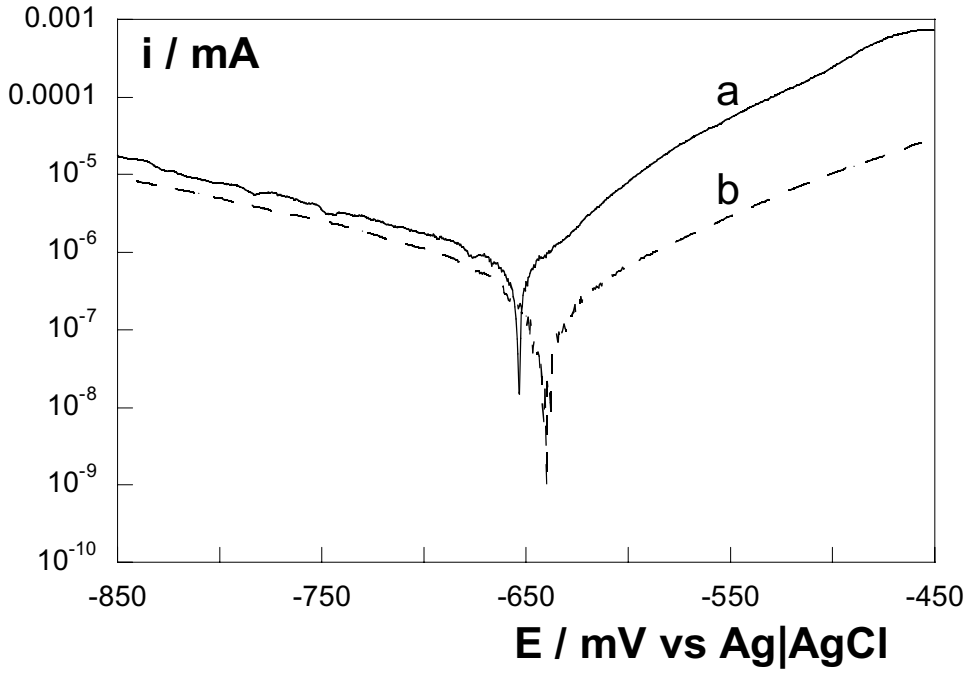

Figure 6. Potentiodynamic polarisation curves in 5% NaCl medium of 2 μm thick (a) Co-11wt% Mo and (b) Co-12wt% Ni-13wt% Mo deposits.

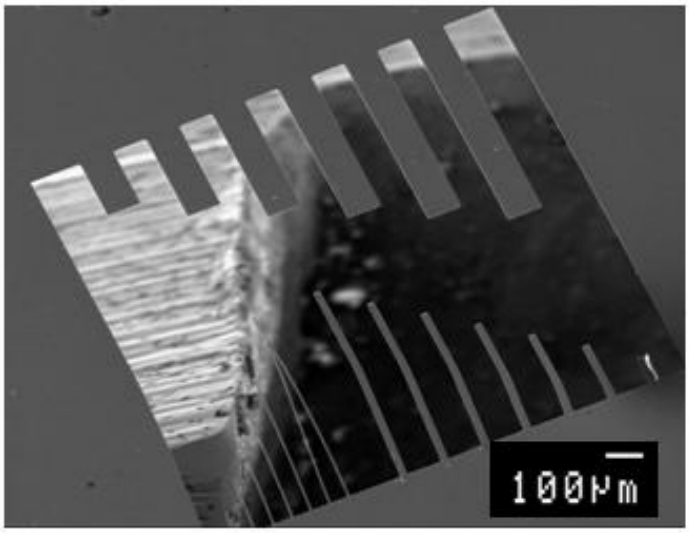

Figure 7. SEM image of a 7 µm thick Co-40wt% Ni test microstructure.

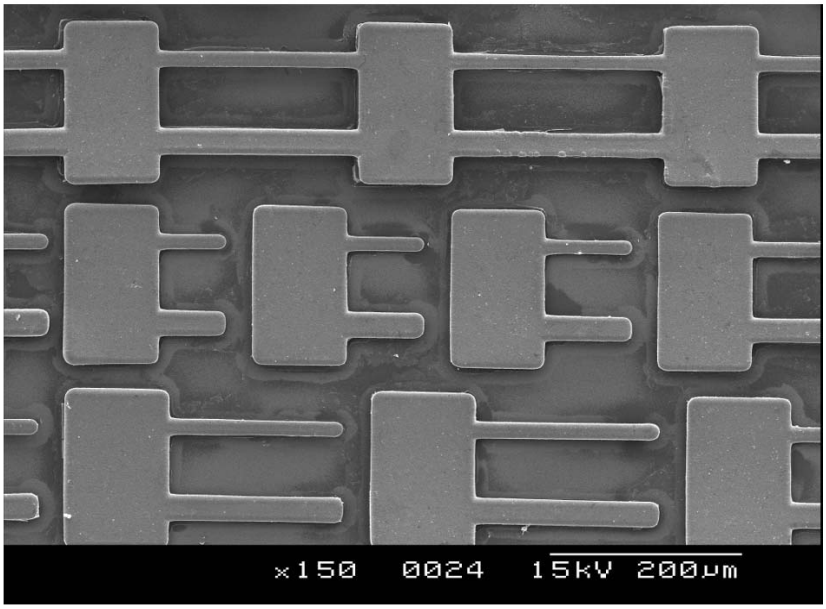

Figure 8. SEM image of released 10 µm thick Co-11wt% Mo microstructures obtained on photolithographed silicon-based substrates.

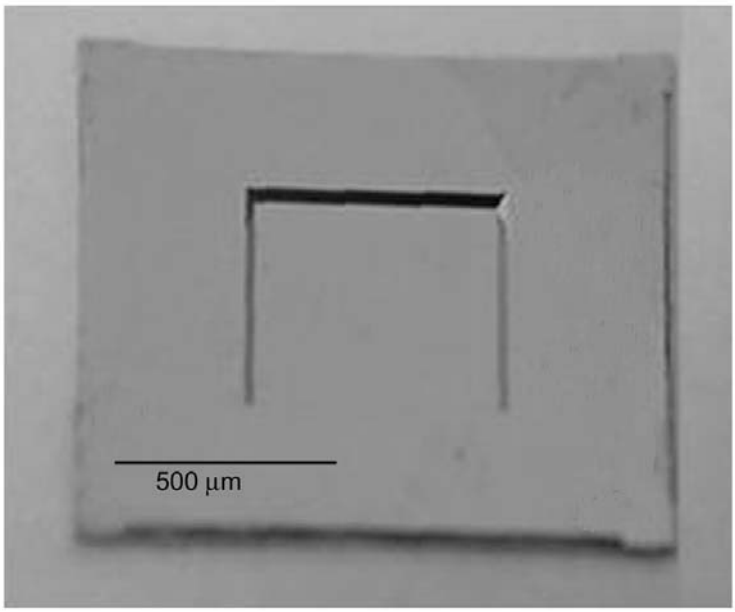

Figure 9. SEM image of a 7 µm thick Co-40wt% Ni membrane with a silicon frame.

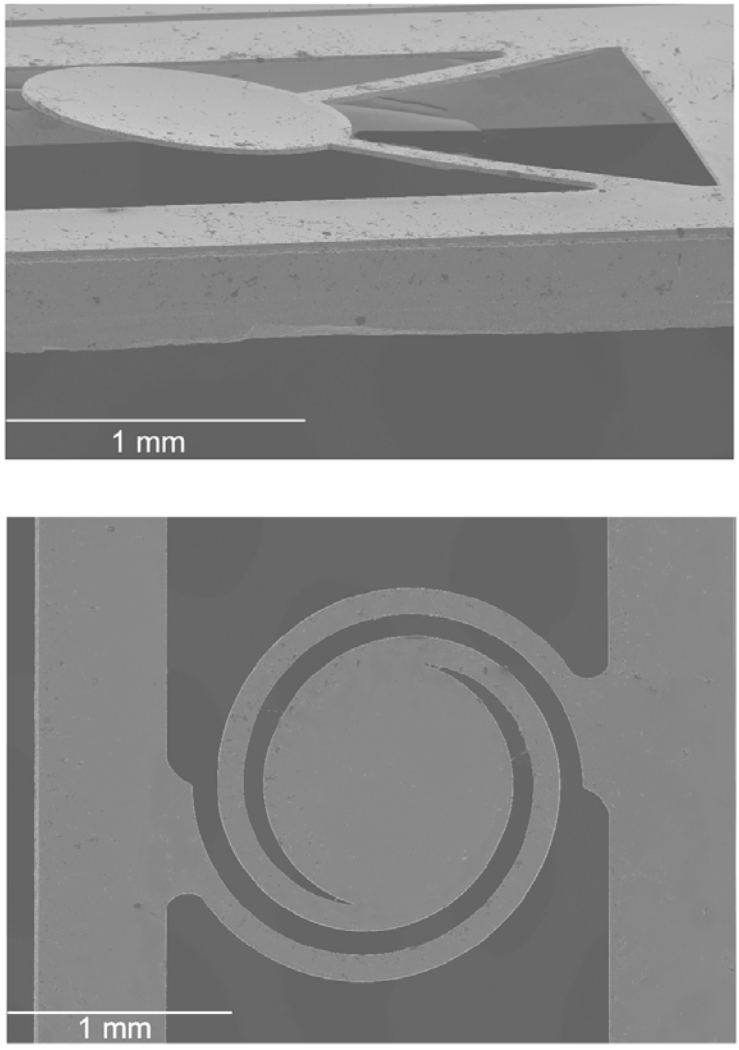

Figure 10. (a) and (b) SEM images of Co-12wt% Ni-13wt% Mo micromachined pieces.